



Validation of the protective effects of *Lonicera japonica* polysaccharide on lipopolysaccharide-induced learning and memory impairments via regulation of autophagy based on network pharmacology

Jiandong Wang¹, Ping Liu², Xiaobo Huang^{1^}, Xiling Wu¹

¹Department of Traditional Chinese Medicine, Xuanwu Hospital, Capital Medical University, Beijing, China; ²School of Pharmacy, Zunyi Medical University, Zunyi, China

Contributions: (I) Conception and design: J Wang; (II) Administrative support: X Huang; (III) Provision of study material: P Liu; (IV) Collection and assembly of data: J Wang, P Liu; (V) Data analysis and interpretation: X Wu; (VI) Manuscript writing: All authors; (VII) Final approval of manuscript: All authors.

Correspondence to: Xiaobo Huang. Department of Traditional Chinese Medicine, Xuanwu Hospital, Capital Medical University, Beijing, China. Email: xiaobohuang123@163.com.

Background: Learning and memory impairments are important indexes in assessing Alzheimer's disease (AD). *Lonicera japonica* (*L. japonica*), a traditional Chinese herbal medicine, inhibits inflammation, but its role in neuroprotection is unclear. Polysaccharide is the main active ingredient in *L. japonica*. Here, we aimed to validate the effects of *L. japonica* polysaccharide (LJP) on lipopolysaccharide (LPS)-induced cognitive impairment and the underlying mechanism.

Methods: The Chinese medicine system pharmacology database and analysis platform was used to predict the target of *L. japonica*; the GeneCards system was used to predict the AD target. We also performed Gene Ontology and Kyoto Encyclopedia of Genes and Genomes (KEGG) pathway enrichment analyses. Experiments were performed after bioinformatic analysis for verification. A chronic learning and memory impairment model was established by a single administration of LPS. Learning and memory abilities of Kunming mice were examined after 7 days of induction. The protective effects of LJP on LPS-induced impairment were investigated. Neuronal damage was observed by Nissl staining. Key proteins involved in the autophagy pathway were examined.

Results: Bioinformatic analysis showed that there were 151 genes in the intersection of the target and AD-related genes, and KEGG analysis suggested that these genes may act via multiple pathways. LPS-induced changes in learning and memory in mice were significantly attenuated by LJP. Nissl staining revealed that the neurons in the control group were lost and cellular arrangement was disrupted. LJP alleviated the pathological changes in the neurons of mice. The autophagy pathway was selected to verify the mechanism. ATG5, Beclin 1, Vps34, and LC3 II expression in the LPS group was significantly increased, and it was further increased in the LJP group.

Conclusions: LJP improved behavioral changes and neuronal loss associated with LPS-induced learning and memory impairments. The underlying mechanism may be related to the regulation of the autophagy pathways.

Keywords: Network pharmacology; *L. japonica* polysaccharide (LJP); lipopolysaccharide (LPS), cognitive impairment; autophagy

Submitted Feb 10, 2020. Accepted for publication Aug 12, 2020.

doi: 10.21037/apm-20-357

View this article at: <http://dx.doi.org/10.21037/apm-20-357>

[^] ORCID: 0000-0001-7495-5035.

Introduction

Alzheimer's disease (AD) is a serious, progressive, neurodegenerative disease that involves irreversible neuronal death leading to cognitive and behavioral impairments (1,2). Globally, over 50 million people are affected by dementia, including AD, and this figure is projected to reach 152 million by 2050 (3). Currently, effective clinical drugs for the treatment of AD are lacking (4). In the past decade, several therapeutic agents have been assessed by clinical trials, but none of them have cleared these trials (5,6).

Autophagy, a basic physiological process, is crucial for cellular homeostasis. A decrease in autophagy efficiency leads to the accumulation of amyloid β ($A\beta$) in the mitochondrial membrane. This event can trigger the caspase cascade, resulting in cell death and neurodegeneration (7). Evidence suggests the accumulation of autophagosomes and high levels of lysosomal hydrolases in the brain of patients with AD, indicating that autophagy may be disrupted (8). Recently, there has been a surge of interest in the mechanisms mediating autophagy. Several regulators are implicated in the main stages of autophagy, such as ATG5, Beclin 1, and class III phosphoinositide 3-kinase Vps34 (9-12). The search and development of autophagy agonists have been the focus of several studies (13-17). Furthermore, the role of autophagy agonists in AD therapy has been widely accepted.

Lonicerajaponica (*L. japonica*), a medicinal plant, has been used for thousands of years in China, mainly for treating influenza, cold, fever, acute rheumatoid arthritis, hepatitis, and infections (18,19). Modern pharmacological studies have shown that *L. japonica* polysaccharide (LJP) extracts exhibit therapeutic potency, including anti-inflammatory (20), antitumor (21), antiviral (22), and anti-oxidant (23) properties. Recent studies have indicated that LJW0F2, a glucan purified from the flowers of *L. japonica*, may block $A\beta$ 42 aggregation and attenuate cytotoxicity in SH-SY5Y cells (24). In a rat model of AD, luteolin, a flavonoid compound derived from *L. japonica*, showed protective effects against $A\beta$ -induced learning and memory impairments via inhibition of oxidative injuries (25). However, the effects of *L. japonica* on lipopolysaccharide (LPS)-induced cognitive impairments remain unknown. Polysaccharide is the main active ingredient in *L. japonica*. In this study, we investigated the pharmacological effects of *L. japonica* using LJP as a representative compound.

In order to further clarify the potential regulatory

effect of *L. japonica* on AD, the possible target genes of *L. japonica* were analyzed using the pharmacological database and analysis platform of the Traditional Chinese Medicine system (TCMSP). The GeneCards system was used to predict disease targets. The intersection genes obtained were analyzed using Cytoscape software to identify the enriched Gene Ontology terms. Furthermore, the Kyoto Encyclopedia of Genes and Genomes (KEGG) pathway enrichment analysis was performed on the acquired genes using the DAVID tool to identify the pathway and functions of the acquired genes.

We performed experimental verification based on the results of the analysis of network pharmacology. We established a cognitive impairment model by intracerebroventricular (i.c.v.) infusion of LPS into mice, followed by LJP treatment. The data obtained revealed that LJP ameliorated learning and memory impairments in a mouse model of LPS-induced AD. Moreover, the data revealed that LJP acted as an autophagy stimulator.

We present the following article in accordance with the ARRIVE reporting checklist (available at <http://dx.doi.org/10.21037/apm-20-357>).

Methods

Drug (L. japonica) and disease (AD) target gene prediction

TCMSP was used to predict the target of *L. japonica*, and the oral bioavailability (OB) was set as >30% and drug similarity (DL) as >0.18 to obtain the gene list. GeneCards (<https://www.genecards.org>) was used to obtain the target protein, using "Alzheimer's disease" as a keyword, and the gene name of the target protein was queried in the Uniprot database.

Intersecting gene acquisition and Venn map drawing

The drug and disease target genes obtained above were imported into Venn (bioinformatics.psb.ugent.be/webtools/Venn) mapping to screen out common gene names to obtain a list of potential target genes for AD treatment with *L. japonica*.

Construction of a protein-protein interaction (PPI) network

Enter the intersection gene in the "Multiple proteins" search box of the STRING (<https://string-db.org>) online

database, adjust the minimum interaction score of the resulting pattern to 0.400, and hide it from the main network. Connect the nodes to show the core target genes. Use barplot to count the number of nodes connected to each node in the network and export its tsv file, import the tsv file into Cytoscape 3.6.1 software to build a “drug-target-disease” network, set various types of nodes to different colors and shapes, and adjust The font size makes it suitable for observation.

KEGG pathway enrichment analysis

The DAVID website (<https://david.ncifcrf.gov>) was used to perform the KEGG pathway enrichment analysis on the intersection target genes. Through the enrichment analysis of functional entries, the biological functions and pathways potentially involving potential LJP targets were investigated, and the pathways with highest potential for treating AD were obtained.

Extraction of LJP

The LJP was prepared according to a previously published method (26,27). The flowers of *L. japonica* (Henan Province, China) were first extracted with ethanol (95%) under reflux for 12 h (in 4 h intervals, thrice) to remove hydrophobic compounds. Then, the remains (approximately 500 g) were extracted with hot distilled water (10 L, 100 °C) twice (4 h each). The extracts were filtered, combined, and concentrated to a final volume of 700 mL. Protein impurities were removed with 15% trichloroacetic acid (4 h, 4 °C). After neutralization, the extracts were placed in 75% absolute ethanol to obtain a precipitate, which was collected and vacuum-dried to obtain LJP (yield 5.1%, w/w).

Animals

Male Kunming mice (6–8 weeks old) were obtained from the Experimental Animal Centre of Army Medical University (Chongqing, China) and used as the experimental model. Each mouse weighed 20±2 g and was maintained under specific pathogen-free conditions. The mice were reared in an animal room maintained at a constant temperature of 25±5 °C and relative humidity of 70%±20% with a 12-h light-dark cycle. The experimental protocol was performed under a project license [No. [2018]-2-122] granted by ethics board of Zunyi Medical University, in compliance with China national or institutional guidelines for the care and

use of animals.

I.c.v. injection of LPS

The mice were treated with the LPS via i.c.v. injection. The mice were anesthetized and placed in a Kopf stereotaxic apparatus (68044; RWD Life Science Inc., Shenzhen, China). An i.c.v. micro-syringe was inserted (A/P -0.2 mm, M/L +1.0 mm, D/V -2.5 mm) unilaterally. The concentration and volume of the LPS solution were 1 mg/mL and 2 µL, respectively. The total i.c.v. infusion time was approximately 10 min.

Establishment of a mouse model of neuroinflammation and drug treatment

The mice are numbered 1–32, 32 serial numbers are randomly numbered, and grouped according to the random number, the mice (n=32) were randomly divided into four groups (control group, LPS group, and LPS + LJP 30 mg/kg and LPS + LJP 100 mg/kg treatment groups) according to their body weight. The dosage of LJP is calculated according to the calculation. The daily dosage of *L. japonica* is about 5 g (brewing), the converted dosage is 0.083 g/kg (calculated by the human weight of 60 kg). According to the yield of LJP 5.1% (w/w), the daily consumption of LJP is 4.16 mg/kg. According to the formula of interspecies body surface area conversion, the equivalent dose of mice is about 37.91 mg/kg, so the dose is set to 30, 100 mg/kg (3-fold relationship).

The mice in the LPS and LPS + LJP groups were injected with LPS (20 µg/mice, i.c.v.). The mice in the LJP groups were administered LJP (i.g.) daily from the day after i.c.v. injection to day 7.

The experimental procedure

Subsequent experiments verified the regulatory effects of the main component of LJP in alleviating learning and memory impairments, an important evaluation index of AD. The experimental procedure is shown in *Figure 1*.

Y-maze behavioral testing

Spatial working memory of mice was tested by spontaneous alternation behavior using the Y-maze. The experimental device of the Y-maze consisted of three arms and one bracket. The angle between each arm was approximately

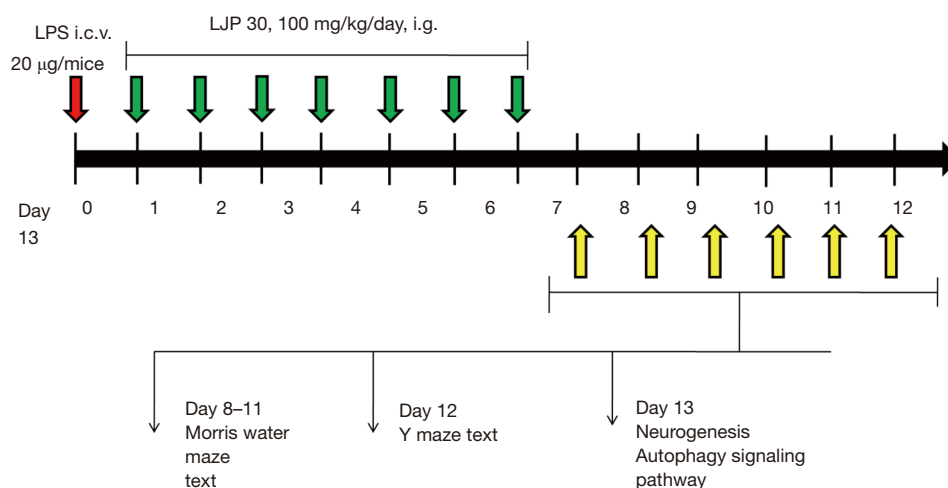


Figure 1 The experimental design. With the exception of mice in the saline group, all mice were injected with LPS (20 µg/mouse, i.c.v.) on day 0. The mice in the LJP groups received LJP (30 or 100 mg/kg, i.g.) from days 1–7. The MWM test was conducted on days 8–11, followed by the Y-maze on day 12. To observe the difference in neurogenesis in the hippocampus of mice and autophagy signaling pathway, Nissl staining and western blotting were performed from day 13. LPS, lipopolysaccharide; i.c.v., intracerebroventricular; LJP, *L. japonica* polysaccharide; *L. japonica*, *Lonicera japonica*; MWM, Morris water maze.

120°. Each arm was 32.5 cm long, the bottom was 8.5 cm wide, and the side baffle was 20 cm high. The ground was not visible to the mice. The stand was 40 cm high and free from the effects of external vibrations. At the beginning of the test, each mouse was placed in the center of the Y-maze. The number and sequence of arm entries within 5 min was recorded. The correct percentage of alternation was calculated. Entering the arm of the maze three times in a row, including entries into all three branches (ABC, ACB, and CAB) was considered a correct alternation. The correct alternation rate was calculated by dividing the number of correct cycles by the maximum number of alternations (total number of entries – 2) × 100. Between tests, the Y-maze was wiped with 70% ethanol to eliminate the effect of odor. Alternation performance above chance level (50%) was indicative of functional spatial working memory (28).

Morris water maze (MWM)

The experimental setup of the MWM consisted of a black circular pool and bracket. The diameter and depth of the pool were 118 and 50 cm, respectively. The pool was divided into four quadrants: southeast, southwest, northeast, and northwest. A movable black platform of diameter 9 cm was placed in the center of the northeast quadrant. The water level was maintained at 0.6–0.8 cm above the water surface,

ensuring that the mice could float but were unable to see the platform under the water. The test water temperature was 22–24 °C. The test was conducted under quiet and dim light conditions. The experiment was divided into two stages: the place navigation test and the space exploration test. The positioning cruise experiment consisted of four training sessions per day for three consecutive days. During training, the mice were placed in the pool from the four starting positions, namely, north, south, east, and west, equidistantly distributed along the edge of the pool, and the mice were free to swim. The training time was 60 s. If a mouse did not find a platform within 60 s, the mouse was placed on the platform for 15 s. If a mouse found the platform unaided within 60 s, it was made to stay there for 15 s by manual control. The mice were removed from the pool and dried immediately. All mice completed a position for one cycle. In total, four cycles were performed per day. Escape latency was recorded (n=8 per group). The space exploration test was set on day 4. The active platform was removed before the test began. The mice were placed in the pool on the opposite quadrant of the platform. The number of times the mice crossed the platform within 60 s was recorded. The experiment was video recorded. Ethovision XT 8.0 (Noldus Information Technology, Wageningen, and the Netherlands) was used to track system records and analyze activity (29).

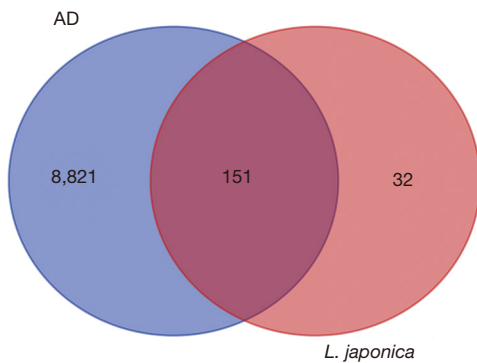


Figure 2 Venn diagram of *L. japonica* and the intersection genes in AD. *L. japonica*, *Lonicera japonica*; AD, Alzheimer's disease.

Pathological observation

Mice anesthetized with sodium pentobarbital (50 mg/kg, i.p.) were transcardially perfused with saline solution followed by 4% paraformaldehyde in phosphate buffer (0.1 M, pH 7.4). The brain was removed, post-fixed overnight in 4% paraformaldehyde at 4 °C, and cut into 4- μ m-thick sections. At 72 h, these sections were deparaffinized, stained with cresyl violet, dehydrated with different concentrations of ethanol, cleared in xylene, and mounted with neutral balsam. Pathological observation and photographing were carried out under a microscope at 200 \times magnifications.

Western blotting

The total protein was extracted from the mouse brain samples. Briefly, tissues were manually homogenized using the RIPA buffer (Cell Signaling Technology, Danvers, MA, USA), in the presence of protease inhibitor (PMSF). Protein concentrations were determined using the bicinchoninic acid method, and equal amounts of protein (30 mg) were separated on 12% SDS-polyacrylamide gels by electrophoresis and then transferred onto polyvinylidene fluoride (PVDF) membranes (Millipore); blocking with 5% non-fat milk was then performed for 1 h. The membranes were then incubated with primary antibodies, including rabbit anti-Atg5 (1:1,000, CST, 12994), rabbit anti-Becn1 (1:1,000, CST, 4122), rabbit anti-Vps34 (1:1,000, CST, 4263), rabbit anti-LC3 II (1:1,000, CST, 3868), and mouse anti- β -actin (1:1,000, Santa Cruz, sc-58679). Following incubation with the appropriate secondary antibodies, the membranes were visualized by chemiluminescence using ECL detection reagents (GE Healthcare Europe GmbH)

and exposed to X-ray films. The results were normalized to the internal control β -actin and the optical density was quantified using Image J.

Statistical analysis

SPSS 22.0 software for Windows (SPSS Inc., Chicago, IL, USA) was used to perform statistical analyses. Experimental data are expressed as mean \pm S.E.M. One-way analysis of variance (ANOVA) was used to compare the differences among three or more groups, with *post hoc* Tukey's test for individual group comparisons. The data of MWM test were analyzed using the two-way ANOVA. A P value <0.05 was set as the level of significance.

Results

Drug-disease target prediction results

The target genes were obtained from the TCMSP database (setting OB >30% and DL >0.18); 8,972 genes were identified. One-hundred and fifty-one protein targets and disease and drug intersection genes were obtained from the GeneCards database (Figure 2).

Construction of the *L. japonica*-AD "drug-target-disease" network

A protein interaction network was constructed using the multiple proteins tool in the STRING online database. The species selected was *Homo sapiens*, the minimum interaction score was set to 0.9, and the disconnected nodes were hidden; the protein interaction map obtained was saved in the TSV format. The information was imported into the Cytoscape 3.6.1 software to illustrate the protein interaction network map to obtain a more concise and clear interaction diagram (Figure 3).

KEGG pathway enrichment analysis

Based on DAVID's online database and R language, the KEGG pathway enrichment analysis was performed to identify potential biological pathways involved in treating AD with *L. japonica*; the mechanism of action of *L. japonica* was explored. The analysis yielded 163 pathways. Autophagy is currently a relevant topic in AD mechanism research; in this study, we noticed a significant change in the autophagy pathway, then map out genes that might be

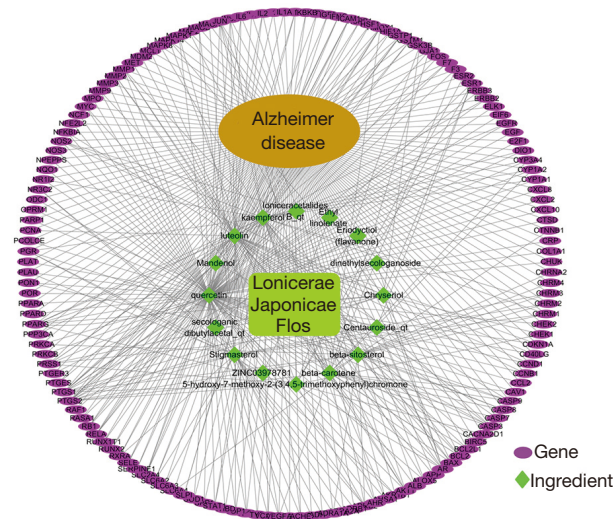


Figure 3 PPI map of *L. japonica* and the intersection genes in AD. PPI, protein-protein interaction; *L. japonica*, *Lonicera japonica*; AD, Alzheimer's disease.

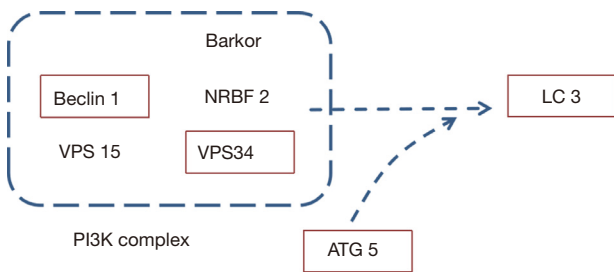


Figure 4 *L. japonica* and the intersection genes in AD enrichment signal pathway autophagy. *L. japonica*, *Lonicera japonica*; AD, Alzheimer's disease.

differentially expressed ($P=0.00268$) (Figure 4).

Effect of LJP on the Y-maze test

In the Y-maze test, each group of mice exhibited a similar number of arm entries (Figure 5A), but there was a significant difference in the alternation of arm entries [$F [3, 21] = 21.45, P < 0.001$]. In post hoc multiple comparisons, the model group administered with LPS exhibited a decreased alternation of arm entries compared with that of the saline group ($P < 0.001$), whereas LJP significantly elevated the alternations compared with that in the model group (100 mg/kg, $P < 0.05$) (Figure 5B).

Effect of LJP on MWM

Place navigation test

Two-way ANOVA was used to analyze the repeated measures of escape latency, and the results revealed that there were significant effects based on training [$F [2, 42] = 18.786, P < 0.01$] and treatment group [$F [3, 21] = 16.284, P < 0.01$], but no significant effect of training \times group [$F [6, 42] = 0.557, P > 0.05$] (Figure 6A,B). The post hoc test (Tukey's HSD) further indicated that the model group showed a significant difference. Escape latency was extended compared with that of the saline group ($P < 0.05$ for day 3). LJP (100 mg/kg) shortened the escape latency after LPS injection ($P < 0.05$ for day 3) (Figure 6C).

The results of the spatial probe test indicated that the recollection of platform location was maintained. There was a significant difference between the groups in platform crossing

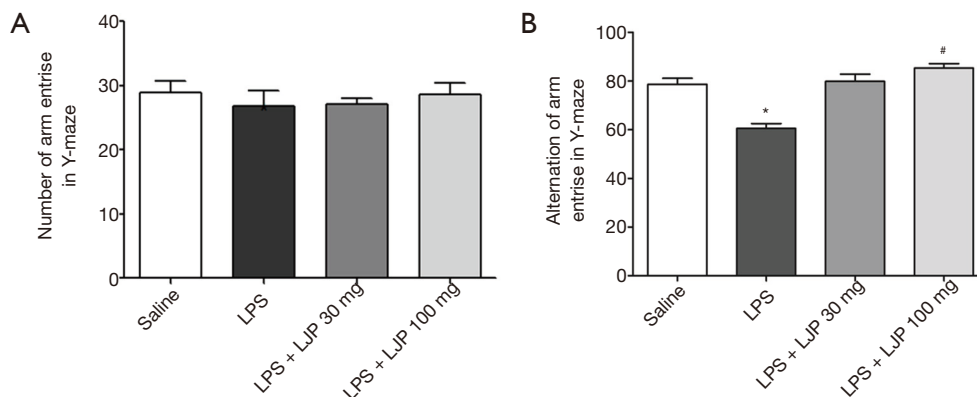


Figure 5 Effects of LJP and LPS on working memory impairment in the Y-maze test. There was no significant difference among the total arm entries in each group (A). Alternation rate was significantly different between groups (B). Data are expressed as mean \pm S.E.M. $n=8$. *, $P < 0.05$ compared with the saline group; #, $P < 0.05$ compared with the LPS group. LJP, *L. japonica* polysaccharide; *L. japonica*, *Lonicera japonica*; LPS, lipopolysaccharide.

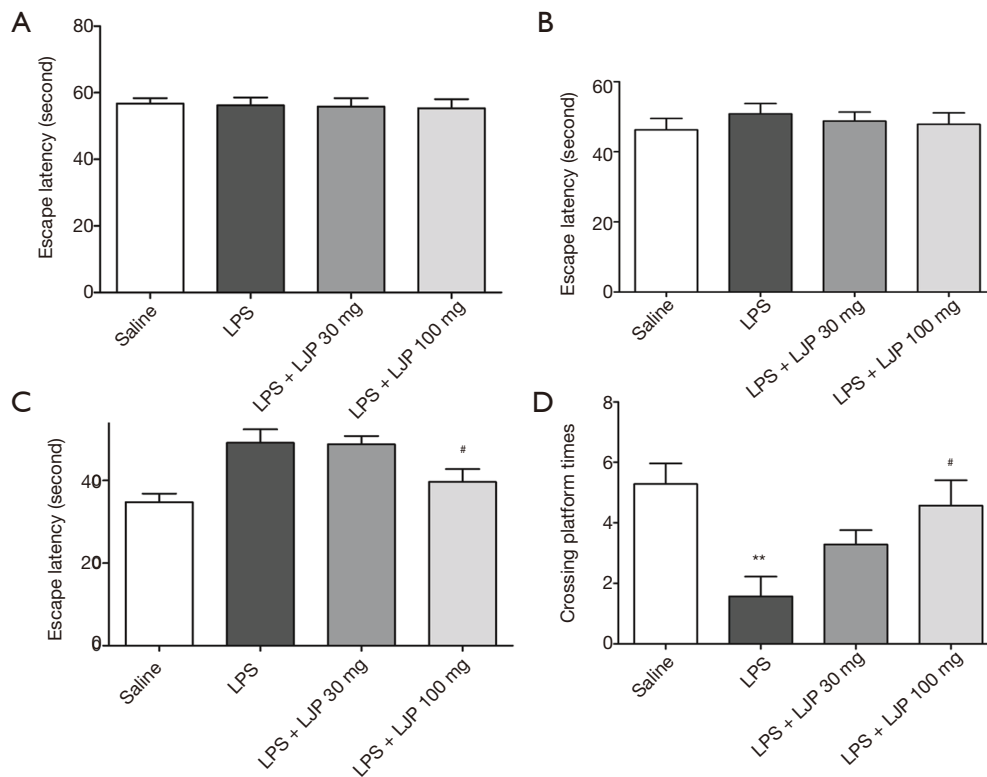


Figure 6 Effects of LJP and LPS on learning and memory impairments in the MWM test. The detection of escape latency on day 1 (A), day 2 (B), and day 3 (C). **, $P < 0.01$ compared with the saline group; #, $P < 0.05$ compared with the LPS group. The detection of crossing between platform times (D). Data are presented as mean \pm S.E.M. *, $P < 0.05$ compared with the saline group. LJP, *L. japonica* polysaccharide; *L. japonica*, *Lonicera japonica*; LPS, lipopolysaccharide; MWM, Morris water maze.

times [F [3, 21] = 0.862, $P < 0.001$]. Tukey's HSD further indicated that treatment with LJP (100 mg/kg) suppressed the reduction in platform crossing times compared with that of the LPS group ($P < 0.05$) (Figure 6D).

Effect of LJP on neurogenesis

In pathological observations, compared with the saline group, samples obtained from the model group exhibited decreased number of neurons in the hippocampus. Neurons were irregularly arranged, deformed, displayed necrosis, and the cell structure was unclear. Samples obtained from the mice in the LJP groups exhibited significantly improved pathology results (Figure 7).

Effects of LJP on autophagy signaling pathway proteins

Key proteins in the autophagy signaling pathway were detected to be involved in the mechanism of action of

LJP. ATG5 is a component of the autophagy complex and an important indicator for the detection of autophagy complexes. The level of ATG5 in the hippocampus was significantly higher in the LPS group than that in the saline group ($P < 0.05$). In the hippocampus of mice administered with the LJP, the ATG5 levels were further elevated (30 mg/kg, $P < 0.05$; 100 mg/kg, $P < 0.01$) (Figure 8A).

Vps34 and Beclin 1 are important components in the autophagosome formation stage and are markers of autophagosome formation. Beclin 1 (Figure 8B) and Vps34 (Figure 8C) levels were significantly elevated in the hippocampus of the model group ($P < 0.05$ and $P < 0.01$, respectively) compared with those in the saline group. In the hippocampus of mice administered 100 mg/kg LJP, the Vps34 levels were further elevated (Beclin 1, $P < 0.05$; Vps34, $P < 0.01$).

The ratio of LC3 II in the hippocampus of the model group was significantly increased ($P < 0.01$). In addition, the ratio of LC3 II was further enhanced after LJP administration

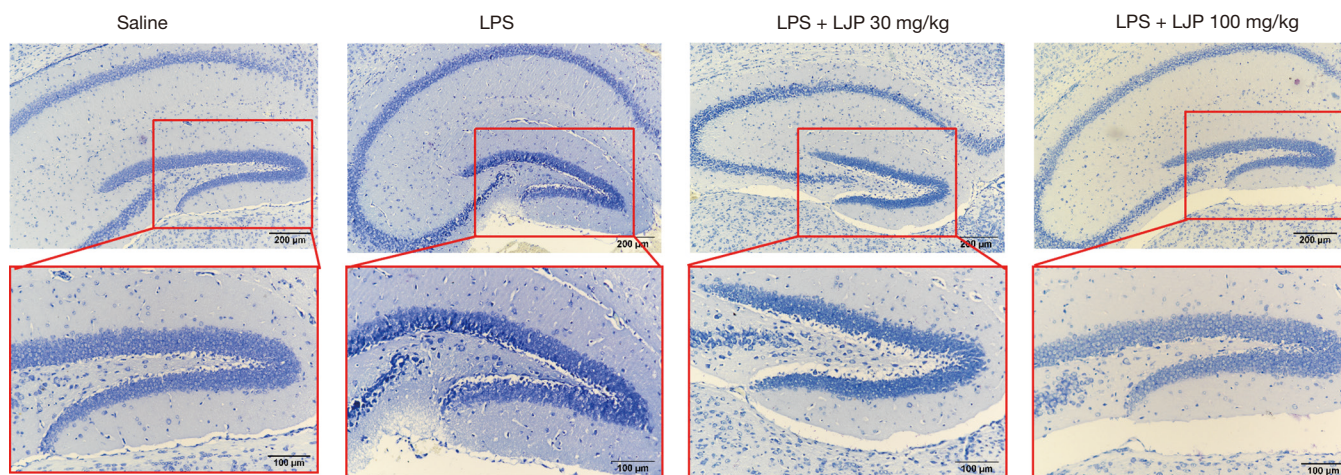


Figure 7 Effect of LJP and LPS on neurogenesis. Observation of mouse neuronal regeneration by Nissl staining. $n=3$. LJP, *L. japonica* polysaccharide; *L. japonica*, *Lonicera japonica*; LPS, lipopolysaccharide.

(30 mg/kg, $P<0.05$, 100 mg/kg, $P<0.01$) (Figure 8D).

Discussion

Network pharmacological prediction experimentally validated models were used in this study. From a macro perspective, network pharmacology evaluates the relationship between drugs and diseases from a multi-component, multi-target, and multi-path point of view. It is an important means in predicting the effect and action mechanism of traditional Chinese medicines and is convenient in their further research. We analyzed *L. japonica* target genes and AD-regulated genes through network pharmacology and explored the possibility of AD treatment with *L. japonica* through gene intersection. We identified 151 intersection genes. Our results suggest that *L. japonica* can be used to treat AD.

Further, enrichment analysis revealed that the target genes may be relevant in regulating multiple signaling pathways. The p value of the autophagy pathway was less than 0.05 ($P=0.00268$), suggesting that it may play an important role. Therefore, we established a mouse model of AD, via intraventricular injection of LPS, to verify the effect of LJP on LPS-induced learning and memory impairment in mice and elucidate the potential action mechanism.

Mice treated with LPS exhibited AD-like symptoms, such as memory decline, abnormal amyloid beta peptide levels, and nicotinic acetylcholine receptors in the brain (30). LPS-induced neuroinflammation models are widely used in AD research (31-33). Qin *et al.* demonstrated

that autophagy is involved in LPS-induced activation of microglial cells, which are clustered around plaques in the brains of rat with AD (34). Luteolin, the major active flavonoid of LJP, protected mice against LPS-induced acute lung injury (35). Our data demonstrated that LJP improved cognitive impairments induced by LPS in mice. This animal study suggested that LJP had beneficial effects against AD symptoms induced by LPS.

AD is characterized by the progressive loss of memory and cognitive abilities, which are correlated with the excessive deposition of extraneuronal A β peptide plaques, intracellular neurofibrillary tangles, and neuronal cell death (36,37). Several herbal medicines have been reported to have potential anti-AD activity (1,38,39). Our results suggested that LJP significantly ameliorated the impairments in spatial learning and working memory of mice, evaluated using the Y-maze and MWM tests. Additionally, mice treated with LJP exhibited significantly improved neuronal injury induced by LPS. These findings suggested that LJP could protect mice with AD against LPS-induced cognitive impairment and neurotoxicity.

Autophagy provides nutrients and macromolecules for cells. The maturation of autophagosomes requires fusion with lysosomes, causing the degradation of autophagosomes, together with its contents. The autophagy-lysosomal system is a chain of events leading to the clearance of misfolded or damaged proteins and dysfunctional organelles (39). Previous research in the neocortex of rat with AD suggested that defects in autophagic maturation may be an important feature of AD pathology. In AD,

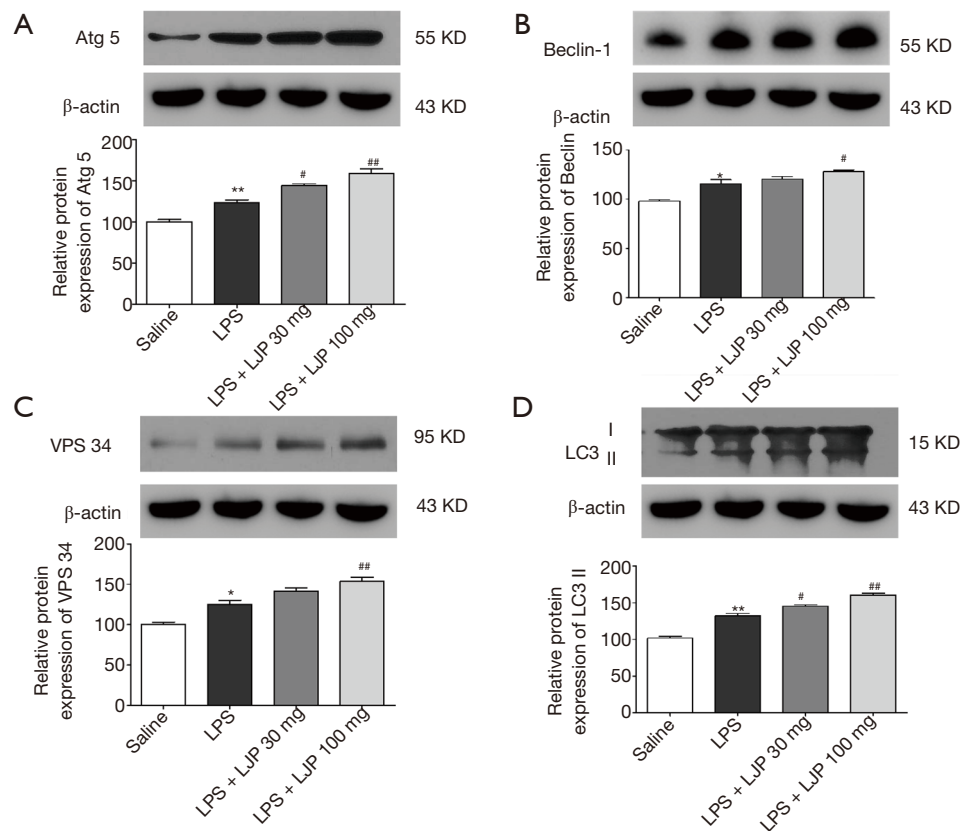


Figure 8 Effects of LJP and LPS on the expression of autophagy-related proteins in the hippocampus of mice. The expression of Atg5 (A), Beclin-1 (B), VPS 34 (C) and LC3 (D). Levels of proteins were quantified using ImageJ software. Data are expressed as means \pm S.E.M., $n=3$. *, $P<0.05$ and **, $P<0.01$ compared with the saline group; #, $P<0.05$ and ##, $P<0.01$ compared with the model group. LJP, *L. japonica* polysaccharide; *L. japonica*, *Lonicera japonica*; LPS, lipopolysaccharide.

autophagy may be impaired during both autophagosome formation and degradation (7,40). Several regulators are implicated in autophagosome formation, such as ATG5, Beclin 1, Vps34, Rab5, and Rab7 (41-46). Our results suggested that LJP administration significantly elevated the expression of LC3 II (a marker of autophagosomes) compared with that in LPS-treated mice. Meanwhile, the levels of ATG5, Beclin 1, and Vps34 were increased in the LJP group. These results suggest that LJP can promote autophagosome formation. However, the effects of LJP on autophagosomes and the degradation of their contents by lysosomes, including autophagosome-lysosome fusion, lysosomal pH, and lysosomal enzyme activities, require further examination. Future research should aim to identify the exact target of LJP.

In summary, we report that LJP significantly improves cognitive impairments induced by LPS. It can activate

autophagy by promoting the formation of autophagosomes. These results highlight the role of LJP as an effective autophagy inducer in the treatment of AD.

Acknowledgments

We wish to thank associate Professor Zhang Tao of Zunyi Medical University donated honeysuckle polysaccharide for this research; We wish to thank the timely help of Editage Insights Ltd. with language touchups.

Funding: This study was supported by the Foundation for Young Scientists Growth Project of Guizhou Province (grant number: qianjiaoheKYzi2017199).

Footnote

Reporting Checklist: The authors have completed the

ARRIVE reporting checklist. Available at <http://dx.doi.org/10.21037/apm-20-357>

Data Sharing Statement: Available at <http://dx.doi.org/10.21037/apm-20-357>

Peer Review File: Available at <http://dx.doi.org/10.21037/apm-20-357>

Conflicts of Interest: All authors have completed the ICMJE uniform disclosure form (available at <http://dx.doi.org/10.21037/apm-20-357>). The authors have no conflicts of interest to declare.

Ethical Statement: The authors are accountable for all aspects of the work and in ensuring that questions related to the accuracy or integrity of any part of the work are appropriately investigated and resolved. Experiments were performed under a project license {No. [2018]-2-122} granted by ethics board of Zunyi Medical University, in compliance with China national or institutional guidelines for the care and use of animals.

Open Access Statement: This is an Open Access article distributed in accordance with the Creative Commons Attribution-NonCommercial-NoDerivs 4.0 International License (CC BY-NC-ND 4.0), which permits the non-commercial replication and distribution of the article with the strict proviso that no changes or edits are made and the original work is properly cited (including links to both the formal publication through the relevant DOI and the license). See: <https://creativecommons.org/licenses/by-nc-nd/4.0/>.

References

- Briggs R, Kennelly SP, O'Neill D. Drug treatments in Alzheimer's disease. *Clin Med (Lond)* 2016;16:247-53.
- Cummings JL, Tong G, Ballard C. Treatment combinations for Alzheimer's disease: current and future pharmacotherapy options. *J Alzheimers Dis* 2019;67:779-94.
- Alzheimer's Disease International. World Alzheimer Report 2018: The state of the art of dementia research: new frontiers. 2018. Available online: <https://www.alz.co.uk/research/WorldAlzheimerReport2018pdf>
- Kabir MT, Uddin MS, Mamun AA, et al. Combination drug therapy for the management of Alzheimer's disease. *Int J Mol Sci* 2020;21:3272.
- Grossberg GT, Tong G, Burke AD, et al. Present algorithms and future treatments for Alzheimer's disease. *J Alzheimers Dis* 2019;67:1157-71.
- Uddin MS, Kabir MT, Jeandet P, et al. Novel anti-Alzheimer's therapeutic molecules targeting amyloid precursor protein processing. *Oxid Med Cell Longev* 2020;2020:7039138.
- Ghavami S, Shojaei S, Yeganeh B, et al. Autophagy and apoptosis dysfunction in neurodegenerative disorders. *Prog Neurobiol* 2014;112:24-49.
- Bordi M, Berg MJ, Mohan PS, et al. Autophagy flux in CA1 neurons of Alzheimer hippocampus: Increased induction overburdens failing lysosomes to propel neuritic dystrophy. *Autophagy* 2016;12:2467-83.
- Deng Q, Wang Z, Wang L, et al. Lower mRNA and protein expression levels of LC3 and Beclin1, markers of autophagy, were correlated with progression of renal clear cell carcinoma. *Jpn J Clin Oncol* 2013;43:1261-8.
- Otomo C, Metlagel Z, Takaesu G, et al. Structure of the human ATG12~ATG5 conjugate required for LC3 lipidation in autophagy. *Nat Struct Mol Biol* 2013;20:59-66.
- Su WC, Chao TC, Huang YL, et al. Rab5 and class III phosphoinositide 3-kinase Vps34 are involved in hepatitis C virus NS4B-induced autophagy. *J Virol* 2011;85:10561-71.
- Uddin MS, Stachowiak A, Mamun AA, et al. Autophagy and Alzheimer's disease: from molecular mechanisms to therapeutic implications. *Front Aging Neurosci* 2018;10:04.
- Fan L, Qiu XX, Zhu ZY, et al. Nitazoxanide, an anti-parasitic drug, efficiently ameliorates learning and memory impairments in AD model mice. *Acta Pharmacol Sin* 2019;40:1279-91.
- Liu Y, Zhou H, Yin T, et al. Quercetin-modified gold-palladium nanoparticles as a potential autophagy inducer for the treatment of Alzheimer's disease. *J Colloid Interface Sci* 2019;552:388-400.
- Martín-Maestro P, Sproul A, Martínez H, et al. Autophagy induction by bexarotene promotes mitophagy in presenilin 1 familial Alzheimer's disease iPSC-derived neural stem cells. *Mol Neurobiol* 2019;56:8220-36.
- Nogalska A, D'Agostino C, Engel WK, et al. Sodium phenylbutyrate reverses lysosomal dysfunction and decreases amyloid- β 42 in an in vitro-model of inclusion-body myositis. *Neurobiol Dis* 2014;65:93-101.
- Ramírez AE, Pacheco CR, Aguayo LG, et al. Rapamycin protects against A β -induced synaptotoxicity by increasing

- presynaptic activity in hippocampal neurons. *Biochim Biophys Acta* 2014;1842:1495-501.
18. Wang C, Wang G, Liu H, et al. Protective effect of bioactive compounds from *Lonicera japonica* Thunb. against H₂O₂-induced cytotoxicity using neonatal rat cardiomyocytes. *Iran J Basic Med Sci* 2016;19:97-105.
 19. Wang T, Yang B, Guan Q, et al. Transcriptional regulation of *Lonicera japonica* Thunb. during flower development as revealed by comprehensive analysis of transcription factors. *BMC Plant Biol* 2019;19:198.
 20. Lee JP, Li YC, Chen HY, et al. Protective effects of luteolin against lipopolysaccharide-induced acute lung injury involves inhibition of MEK/ERK and PI3K/Akt pathways in neutrophils. *Acta Pharmacol Sin* 2010;31:831-8.
 21. Park C, Lee WS, Han MH, et al. *Lonicera japonica* Thunb. Induces caspase-dependent apoptosis through death receptors and suppression of AKT in U937 human leukemic cells. *Phytother Res* 2018;32:504-13.
 22. Ding Y, Cao Z, Cao L, et al. Antiviral activity of chlorogenic acid against influenza A (H1N1/H3N2) virus and its inhibition of neuraminidase. *Sci Rep* 2017;7:45723.
 23. Chaowuttikul C, Palanuvej C, Ruangrunsi N. Pharmacognostic specification, chlorogenic acid content, and in vitro antioxidant activities of *Lonicera japonica* flowering bud. *Pharmacognosy Res* 2017;9:128-32.
 24. Wang P, Liao W, Fang J, et al. A glucan isolated from flowers of *Lonicera japonica* Thunb. inhibits aggregation and neurotoxicity of A β 42. *Carbohydr Polym* 2014;110:142-7.
 25. Yu TX, Zhang P, Guan Y, et al. Protective effects of luteolin against cognitive impairment induced by infusion of A β peptide in rats. *Int J Clin Exp Pathol* 2015;8:6740-7.
 26. Zhang T, Xiang J, Zheng G, et al. Preliminary characterization and anti-hyperglycemic activity of a pectic polysaccharide from okra (*Abelmoschus esculentus* (L.) Moench). *J Funct Foods* 2018;41:19-24.
 27. Liu P, Bai X, Zhang T, et al. The protective effect of *Lonicera japonica* polysaccharide on mice with depression by inhibiting NLRP3 inflammasome. *Ann Transl Med* 2019;7:811.
 28. Hou Y, Xie G, Miao F, et al. Pterostilbene attenuates lipopolysaccharide-induced learning and memory impairment possibly via inhibiting microglia activation and protecting neuronal injury in mice. *Prog Neuropsychopharmacol Biol Psychiatry* 2014;54:92-102.
 29. Zhou J, Yu W, Zhang M, et al. Imbalance of microglial TLR4/TREM2 in LPS-treated APP/PS1 transgenic mice: a potential link between Alzheimer's disease and systemic inflammation. *Neurochem Res* 2019;44:1138-51.
 30. Lykhmus O, Uspenska K, Koval L, et al. N-Stearoylethanolamine protects the brain and improves memory of mice treated with lipopolysaccharide or immunized with the extracellular domain of α 7 nicotinic acetylcholine receptor. *Int Immunopharmacol* 2017;52:290-6.
 31. Zakaria R, Wan Yaacob WM, Othman Z, et al. Lipopolysaccharide-induced memory impairment in rats: a model of Alzheimer's disease. *Physiol Res* 2017;66:553-65.
 32. Andy SN, Pandey V, Alias Z, et al. Deoxyephantopin ameliorates lipopolysaccharides (LPS)-induced memory impairments in rats: evidence for its anti-neuroinflammatory properties. *Life Sci* 2018;206:45-60.
 33. Singh R, Thota S, Bansal R. Studies on 16,17-pyrazoline substituted heterosteroids as anti-Alzheimer and anti-Parkinsonian agents using LPS induced neuroinflammation models of mice and rats. *ACS Chem Neurosci* 2018;9:272-83.
 34. Qin C, Liu Q, Hu ZW, et al. Microglial TLR4-dependent autophagy induces ischemic white matter damage via STAT1/6 pathway. *Theranostics* 2018;8:5434-51.
 35. Cameron DJ, Galvin C, Alkam T, et al. Alzheimer's-related peptide amyloid- β plays a conserved role in angiogenesis. *PLoS One* 2012;7:e39598.
 36. Sereia AL, de Oliveira MT, Baranoski A, et al. In vitro evaluation of the protective effects of plant extracts against amyloid-beta peptide-induced toxicity in human neuroblastoma SH-SY5Y cells. *PLoS One* 2019;14:e0212089.
 37. Yao XC, Xue X, Zhang HT, et al. Pseudoginsenoside-F11 alleviates oligomeric β -amyloid-induced endosome-lysosome defects in microglia. *Traffic* 2019;20:61-70.
 38. Farkhondeh T, Samarghandian S, Pourbagher-Shahri AM, et al. The impact of curcumin and its modified formulations on Alzheimer's disease. *J Cell Physiol* 2019;234:16953-65.
 39. Zare-Shahabadi A, Masliah E, Johnson GV, et al. Autophagy in Alzheimer's disease. *Rev Neurosci* 2015;26:385-95.
 40. Arroyo DS, Gaviglio EA, Peralta Ramos JM, et al. Autophagy in inflammation, infection, neurodegeneration and cancer. *Int Immunopharmacol* 2014;18:55-65.
 41. Agola JO, Jim PA, Ward HH, et al. Rab GTPases as regulators of endocytosis, targets of disease and therapeutic opportunities. *Clin Genet* 2011;80:305-18.
 42. Chen Y, Zhou F, Zou S, et al. A Vps21 endocytic module

- regulates autophagy. *Mol Biol Cell* 2014;25:3166-77.
43. He C, Klionsky DJ. Regulation mechanisms and signaling pathways of autophagy. *Annu Rev Genet* 2009;43:67-93.
 44. Hyttinen JM, Niittykoski M, Salminen A, et al. Maturation of autophagosomes and endosomes: a key role for Rab7. *Biochim Biophys Acta* 2013;1833:503-10.
 45. Jäger S, Bucci C, Tanida I, et al. Role for Rab7 in maturation of late autophagic vacuoles. *J Cell Sci* 2004;117:4837-48.
 46. Poteryaev D, Datta S, Ackema K, et al. Identification of the switch in early-to-late endosome transition. *Cell* 2010;141:497-508.

Cite this article as: Wang J, Liu P, Huang X, Wu X. Validation of the protective effects of *Lonicera japonica* polysaccharide on lipopolysaccharide-induced learning and memory impairments via regulation of autophagy based on network pharmacology. *Ann Palliat Med* 2021;10(2):1089-1100. doi: 10.21037/apm-20-357